Keywords
Triple-negative breast cancer, Casein Kinase 2 alpha, Nicotiflorin, Molecular docking, In vitro evaluation, In vivo toxicity

Authors
Diksha Dube[1*]
Department of Pharmacology, Rashtrasant Janardhan Swami College of Pharmacy, Kokamthan, Maharashtra, India. Email: dikshadube2001@gmail.com.

Dr. Nitin Jain[2]
Department of Pharmaceutical Chemistry, Rashtrasant Janardhan Swami College of Pharmacy, Kokamthan, Maharashtra, India

Mr. Prasanna Dalvi[3]
Department of Pharmacology, Rashtrasant Janardhan Swami College of Pharmacy, Kokamthan, Maharashtra, India

Pratiksha Udawant[4]
Department of Pharmacology, Rashtrasant Janardhan Swami College of Pharmacy, Kokamthan, Maharashtra, India

Shweta Pati[5]
Department of Pharmacology, Rashtrasant Janardhan Swami College of Pharmacy, Kokamthan, Maharashtra, India

Pratiksha Vadhane[6]
Department of Pharmacology, Rashtrasant Janardhan Swami College of Pharmacy, Kokamthan, Maharashtra, India

Usha Jain[7]
Vice Principal, Associate Professor, Pharmaceutical Chemistry, Rashtrasant Janardhan Swami College of Pharmacy Kokamthan, Email Id: unjain11@gmail.com

Received-14-06-2026
Revised-17-07-2026
Accepted-20-07-20.26
Doi:10.1922/ejprd.v34i5s.1525

Drug Discovery and Bioassay Screening for Triple-Negative Breast Cancer: Identification and Evaluation of Nicotiflorin as a Casein Kinase 2 Alpha Inhibitor

Abstract
Triple-negative breast cancer (TNBC) is an aggressive subtype lacking hormone receptors and HER2 expression, with limited therapeutic options. Casein Kinase 2 alpha (CK2α) is implicated in TNBC progression and represents a promising drug target. This study integrates in silico molecular docking, ADME profiling, in vitro anticancer assays, and in vivo acute toxicity evaluation to identify and validate Nicotiflorin, a natural flavonoid, as a potent CK2α inhibitor. Molecular docking and dynamics simulations showed strong binding affinity and complex stability. Nicotiflorin significantly inhibited viability, migration, and colony formation of MDA-MB-231 TNBC cells, with minimal toxicity to normal HEK-293 and BALB 3T3 cells. Acute oral toxicity studies in Wistar albino rats demonstrated a favorable safety profile. These results suggest Nicotiflorin as a promising lead compound for TNBC therapy targeting CK2α.

INTRODUCTION

Breast cancer remains the leading cause of oncogenic morbidity and mortality among women globally [1]. Based on distinct gene expression profiles, this highly heterogeneous disease is classified into specific molecular subtypes: Luminal A, Luminal B, HER2-enriched, and Triple-Negative Breast Cancer (TNBC) [2]. TNBC accounts for approximately 15–20% of all breast cancer diagnoses and represents a highly aggressive, invasive clinical phenotype. It is defined by the absolute absence of estrogen receptor (ER) expression, progesterone receptor (PR) expression, and human epidermal growth factor receptor 2 (HER2) amplification [2,3]. The absence of these molecular targets severely limits conventional endocrine or HER2-directed therapies, culminating in a exceptionally poor prognosis [3]. Histologically, TNBC typically presents as high-grade carcinomas characterized by central necrotic zones, prominent lymphocytic stromal infiltration, and pushing invasion borders [4]. Clinically, patients suffer from abbreviated progression-free survival (PFS), diminished overall survival (OS), and early visceral recurrence [4]. At the genomic level, next-generation sequencing (NGS) has unveiled profound transcriptomic heterogeneity within TNBC, leading to its stratification into six distinct ontogenic subtypes: Basal-like 1 (BL1), Basal-like 2 (BL2), Immunomodulatory (IM), Mesenchymal (M), Mesenchymal Stem-Like (MSL), and Luminal Androgen Receptor (LAR) [5-7].

MATERIALS AND IN SILICO METHODOLOGY:

MATERIALS

The present investigation integrated computational, in vitro, and in vivo approaches to evaluate the anticancer potential of Nicotiflorin against triple-negative breast cancer (TNBC). All chemicals and reagents employed in the study were of analytical or cell culture grade and were procured from authenticated commercial suppliers. Cell culture experiments were conducted under sterile laboratory conditions using validated equipment and standard operating procedures.

Software, Web Servers, and Databases

The computational workflow incorporated publicly accessible databases and validated molecular modeling software for protein retrieval, ligand preparation, molecular docking, molecular dynamics simulations, pharmacokinetic prediction, and toxicity assessment. These platforms facilitated target identification, molecular interaction analysis, and prediction of the physicochemical and pharmacological properties of Nicotiflorin.

Table 1. Software, web tools, and databases used in the study.

SR. NO.	SOFTWARE NAME	ACCESS LINK
1	RCBS-PDB Datebase	https://www.rcsb.org/
2	PubChem Databse	https://pubchem.ncbi.nlm.nih.gov/
3	UCSF- Chimera	https:/ / www.cgl.ucsf.edu/ chimera/
4	PyRx (8.0)	https://pyrx.sourceforge.io/
5	Swiss- ADME	http://www.swissadme.ch/
6	Data Warrior	https://openmolecules.org/datawarrior/
7	Protox II	https://tox.charite.de/protox3/
8	Open Bable 2.4.1	https:/ / sourceforge.net/ projects/ openbabel/
9	Discovery Studio Visualizer	https:/ / discover.3ds.com/ discovery-studio-visualizer-
10	MagVision	https:/ / www.olympus- lifescience.com/ en/support/downloads
11	Prism 8	https:/ / wsr.imagej.net/ distros/ win/ ij154-win-java8.zip
12	Sklant 7. RE	
13	Image J	https:/ / wsr.imagej.net/ distros/ win/ ij154-

Chemicals

Analytical-grade chemicals and cell culture reagents were utilized throughout the experimental work. Cell culture media, fetal bovine serum (FBS), antibiotics, MTT reagent, Trypan Blue, dimethyl sulfoxide (DMSO), crystal violet,

glutaraldehyde, and other reagents were obtained from certified manufacturers and prepared according to the manufacturers' recommendations to ensure experimental reproducibility.

Table 2. List of chemicals

Sr. No.	Material
1	Antibiotic- Antimycotic Solution (100x) [A5955]
2	Crystal Violet dye
3	Dimethyl Sulphoxide [Cash no. 676805]
4	Dimethyl Sulphoxide Cell Culture Tested [TC185]
5	Doxorubicin
6	Dulbecco's Phospate Buffred Saline 1X [TL1023]
7	Ethanol, absolute [UN No:1170].
8	Fetal Bovine Serum- USDA Approved [RM9952]
9	Glutaraldehyde solution
10	Leibovitz's L-15 Media [AL011S]
11	Methotrexate Anticancer drug
12	Minimum Essential Media Eagle [AT047]
13	Molecular Biology Grade Water (DEPC-Treated) [ML024]
14	MTT dye [RM1131]
15	Trypan Blue 0.5% solution in PBS [TCL005]
16	Trypsin -EDTA solution [TCL-152]
17	Water- HPLC and Spectroscopy [SAP Code-31930LC100]

Instruments and Equipment

Experimental procedures were performed using calibrated laboratory instruments, including biosafety cabinets, CO_2 incubators, ELISA plate readers, inverted microscopes, analytical balances, micropipettes, and scanning electron microscopy facilities. All instruments were operated according to institutional quality assurance guidelines.

Table 3. List of equipment

SR.No.	Name of Equipment	Name of Manufacturing and Model
1.	Biosafety Cabinet Class-II	Esco, Singapore
2.	CO2 Incubator	RS Biotech, Mini Galaxy A, Scotland
3.	Deep Freezer	Dairei, Denmark
4.	Digital Analytical Balance	Endel (EJB- FE300)
5.	ELISA Plate Reader	Thermo, USA
6.	Micro Plate Reader	Thermo Scientific
7.	Micropipettes	Eppendorf, Germany
8.	RO Water System	Milipore, USA
9.	Scanning Electron Microscopy	Nova Nano SEM NPEP 303

Glassware and Plasticware

Sterile disposable plasticware and borosilicate glassware were employed for all laboratory procedures involving cell culture, biochemical assays, and molecular analyses. All reusable materials were sterilized before experimental use to minimize contamination.

Table 4. Glassware and plasticware

Sr. No.	Glassware
1	Beaker
2	Cell counting Chamber-Hemocytometer
3	Cell Scraper
4	Cotton
5	Flacon Tube
6	Glass Cover Slip
7	Measuring Cylinder
8	Microtiter Plate- 96, 12, 6
9	Micropipette tips
10	Multi-channel pipette tray
11	Petri dish
12	Reagent bottles (100ml, 250ml, 500ml)
13	Single and multi-channel micropipette
14	Small-Eppendorf tube
15	Sterile plasticware
16	T-Flask [Vented and Canted]

Cell Lines

Three authenticated mammalian cell lines were used to investigty ate the anticancer efficacy and cytotoxic profile of Nicotiflorin. The human triple-negative breast cancer cell line MDA-MB-231 served as the experimental cancer model, whereas BALB/3T3 Clone A31 and HEK-293 cells were employed for evaluating cytotoxicitoward normal mammalian cells.

Table 5. Cell lines used in the study

Sr. No	Cancer and Normal Cell Line	Types of Cells
1.	MDA- MB-231	Triple Negative Breast Cancer
2.	BALB 3T3 Clone A31	Mouse Embryonic Fibroblast
4.	HEK	Human Kidney Normal Cell Line

In Silico Studies

Computational Environment

Computational investigations were performed on a high-performance workstation equipped with an Intel® Xeon® W-2155 processor, NVIDIA Quadro RTX 6000 graphics processor, 128 GB RAM, and an 8 TB storage drive operating under Ubuntu 22.04 LTS. This hardware configuration enabled efficient execution of molecular docking, molecular dynamics simulations, and free-energy calculations while ensuring computational stability and reproducibility.

Protein Retrieval

The crystallographic structure of Casein Kinase 2 (CK2α) was retrieved from the Research Collaboratory for Structural Bioinformatics Protein Data Bank (RCSB-PDB). The selected structure (PDB ID: 4KWP) corresponds to the human CK2 protein with a crystallographic resolution of 1.25 Å, providing a highly reliable structural template for molecular docking studies. The structure was downloaded in Protein Data Bank (PDB) format and subsequently processed for receptor preparation (RCSB Protein Data Bank, 2025).

Table 6. Structural characteristics of the selected protein

Parameter	Description
Protein	Casein Kinase 2
PDB ID	4KWP
Organism	Homo sapiens

Classification	Transferase
Resolution	1.25 Å
Mutation	None

Protein Preparation

The retrieved CK2 crystal structure underwent comprehensive preprocessing using the Protein Preparation Wizard available in Schrödinger Maestro (version 2024-1). Protein optimization involved correcting bond orders, assigning appropriate ionization states, addition of hydrogen atoms, removal of crystallographic water molecules distant from the active site, and elimination of irrelevant heteroatoms. Missing side chains and loop regions were reconstructed using the Prime module to improve structural completeness. Subsequently, restrained energy minimization was performed using the OPLS4 force field until an RMSD convergence threshold of 0.30 Å was achieved. These procedures generated an energetically optimized receptor suitable for molecular docking and dynamic simulations (Friesner et al., 2004; Harder et al., 2016).

Ligand Preparation

The three-dimensional chemical structure of Nicotiflorin was obtained from the PubChem database in SDF format. Ligand optimization was carried out using the LigPrep module of Schrödinger. Protonation states were generated at physiological pH (7.4 ± 0.5) using the Epik algorithm. Salt forms were removed, stereochemical configurations were preserved, and energetically favorable tautomers were generated. Final geometry optimization was performed with the OPLS4 force field to obtain biologically relevant conformations suitable for molecular docking (Harder et al., 2016).

Molecular Docking

Molecular docking was performed using the Glide Extra Precision (XP) algorithm implemented in Schrödinger Maestro. The receptor grid was generated by defining the active-site region around the co-crystallized ligand. Default van der Waals scaling parameters and partial charge cut-offs were applied during receptor grid generation.

Prepared ligand conformations were flexibly docked into the receptor binding pocket. During docking, Epik state penalties and non-planar amide penalties were incorporated into the scoring function to improve prediction accuracy. Following docking, ligand poses were energy-minimized, and binding affinities were ranked according to GlideScore values. The binding orientation exhibiting the lowest docking score and most favorable intermolecular interactions was selected for subsequent molecular dynamics simulations (Friesner et al., 2004).

Molecular Dynamics (MD) Simulation

To investigate the dynamic stability of the docked protein–ligand complexes under physiological conditions, molecular dynamics (MD) simulations were carried out using the Desmond simulation package integrated within the Schrödinger software suite. The three receptor–ligand complexes exhibiting the most favorable docking scores were selected for simulation analysis.

Each complex was embedded in an orthorhombic simulation box containing SPC water molecules, maintaining a minimum distance of 10 Å between the protein surface and the box boundaries. The systems were neutralized by adding appropriate sodium (Na^+) counterions, followed by supplementation with 0.15 M sodium chloride (NaCl) to reproduce physiological ionic strength. Energy minimization and system equilibration were subsequently performed using the OPLS4 force field before initiating the production simulation.

Production simulations were conducted for 100 ns under the NPT ensemble, maintaining constant temperature (310 K) and pressure (1.01325 bar). Trajectory data were recorded at regular intervals to monitor structural and conformational changes throughout the simulation period.

The stability of each protein–ligand complex was evaluated by analyzing root mean square deviation (RMSD), root mean square fluctuation (RMSF), protein–ligand interaction profiles, radius of gyration (Rg), hydrogen bond occupancy, and secondary structural stability. These parameters collectively provided insight into the conformational behavior and binding stability of Nicotiflorin within the active site of CK2 (Bowers et al., 2006; Harder et al., 2016).

Binding Free Energy Estimation Using Prime MM-GBSA

The binding affinity of Nicotiflorin toward Casein Kinase 2 was further quantified using the Prime Molecular Mechanics–Generalized Born Surface Area (MM-GBSA) approach available in Schrödinger. This method estimates the thermodynamic stability of receptor–ligand complexes by integrating molecular mechanics energies with implicit solvation effects.

Binding free energy (ΔG_bind) was determined using the following equation:

$$\Delta G_{bind} = G_{complex} - (G_{protein} + G_{ligand})$$

where:

- $G_{complex}$ = Free energy of the protein–ligand complex
- $G_{protein}$ = Free energy of the isolated receptor
- G_{ligand} = Free energy of the isolated ligand

Representative conformations extracted from the MD trajectories were analyzed using the VSGB 2.0 implicit solvation model. Binding free energies were calculated at regular intervals from the equilibrated phase of the simulation to estimate the average binding affinity and energetic stability of the complexes (Li et al., 2011).

In Vitro Studies

Cell Culture

Human triple-negative breast cancer (MDA-MB-231) cells and murine embryonic fibroblast (BALB/3T3 Clone A31) cells were obtained from the National Centre for Cell Science (NCCS), Pune, India. Human embryonic kidney (HEK-293) cells were used to evaluate cytotoxicity toward normal cells.

MDA-MB-231 cells were cultured in Leibovitz's L-15 medium, whereas BALB/3T3 and HEK-293 cells were maintained in Dulbecco's Modified Eagle Medium (DMEM). Culture media were supplemented with 10% fetal bovine serum (FBS) and 1% antibiotic–antimycotic solution containing penicillin and streptomycin.

Cells were incubated at 37°C in a humidified atmosphere containing 5% CO_2 until they reached approximately 80–90% confluence. Culture media were replaced every 48–72 h, and cells were subcultured using trypsin–EDTA according to standard cell culture procedures (Freshney, 2016).

Cell Viability Assessment

Cell viability was determined using the Trypan Blue exclusion assay, which differentiates viable cells from membrane-compromised non-viable cells. Equal volumes of cell suspension and 0.4% Trypan Blue solution were mixed and incubated at room temperature for approximately 3 min before loading onto a hemocytometer.

Cells were counted under an inverted microscope, and viable (unstained) and non-viable (blue-stained) cells were recorded separately. Cell concentration and percentage viability were calculated using the following equations:

Cells/mL= Average cell count×Dilution factor×104 /Number of squares counted

Cell Viability (%)=Number of viable cells/Total number of cells×100

This procedure was performed before every cytotoxicity experiment to ensure uniform cell seeding and reproducibility (Strober, 2015).

MTT Cytotoxicity Assay

The antiproliferative activity of Nicotiflorin against MDA-MB-231 cells was assessed using the MTT colorimetric assay, which measures mitochondrial metabolic activity as an indicator of viable cells (Mosmann, 1983).

Cells were seeded into sterile 96-well microplates and allowed to attach overnight. Following incubation, the cultures were exposed to increasing concentrations of Nicotiflorin for 24 h. After treatment, 20 µL of MTT reagent was added to each well, and the plates were incubated for an additional 4–5 h at 37°C to allow intracellular reduction of MTT into insoluble purple formazan crystals.

The culture medium was carefully removed, and the crystals were dissolved using 100 µL DMSO. Absorbance was measured at 570 nm using a microplate reader. Untreated cells served as the negative control, whereas Doxorubicin was used as the positive control.

Percentage inhibition of cell growth was calculated as follows:

$$\% \text{ Inhibition} = OD_{control} - OD_{treated} / OD_{control} \times 100$$

Dose–response curves were generated using GraphPad Prism, and IC_{50} values were calculated by nonlinear regression analysis.

Cytotoxicity Assessment on Normal Cell Line (HEK-293)

The cytotoxic potential of Nicotiflorin toward normal cells was evaluated using the human embryonic kidney cell line (HEK-293) to determine its safety profile. HEK-293 cells obtained from the National Centre for Cell Science (NCCS), Pune, were cultured in Dulbecco's Modified Eagle Medium (DMEM) supplemented with 10% fetal bovine serum and 1% antibiotic-antimycotic solution under standard incubation conditions (37°C, 5% CO_2).

Cells were seeded into 96-well culture plates at an appropriate density and incubated for 24 h to allow cell attachment. Nicotiflorin was dissolved in dimethyl sulfoxide (DMSO) to prepare a stock solution (1 mg/mL), followed by serial dilutions to obtain the required treatment concentrations. After 24 h of exposure, cell viability was determined using the MTT assay. Briefly, MTT reagent was added to each well and incubated for 3 h to facilitate intracellular formation of formazan crystals by metabolically active cells. The culture medium was carefully removed, and the crystals were dissolved using DMSO. Absorbance was measured at 570 nm using a microplate reader, and cell viability was expressed relative to untreated control cells. The assay was performed in triplicate to ensure experimental reproducibility (Mosmann, 1983).

Neutral Red Uptake Assay

The Neutral Red Uptake (NRU) assay was performed to evaluate lysosomal integrity and determine the cytotoxicity of Nicotiflorin in BALB/3T3 fibroblast cells. Cells were seeded in 96-well plates and allowed to adhere overnight before treatment with serial concentrations of the test compound prepared from a 1 mg/mL stock solution.

Following 48 h of incubation, the culture medium was replaced with Neutral Red solution (25 µg/mL), and the cells were incubated for an additional 3 h. Excess dye was removed by washing with phosphate-buffered saline, and the incorporated dye was extracted using a freshly prepared desorption solution containing ethanol, distilled water, and glacial acetic acid. Absorbance was recorded at 540 nm using a microplate reader. Cytotoxicity was expressed as the percentage of viable cells relative to untreated controls, and the median lethal dose (LD_{50}) was estimated using the established regression equation (Borenfreund & Puerner, 1985).

Clonogenic Assay

The long-term antiproliferative effect of Nicotiflorin was assessed using a clonogenic survival assay. MDA-MB-231 cells were seeded in six-well culture plates at a low density (approximately 1×10^3 cells per well) and incubated overnight to allow cell attachment. The cells were subsequently treated with different concentrations of Nicotiflorin and maintained under standard culture conditions for seven days to permit colony formation.At the end of the incubation period, colonies were fixed with 6% glutaraldehyde and stained with 0.5% crystal violet. Colonies consisting of at least 50 cells were

considered viable and were photographed using an inverted microscope. Colony numbers were quantified to determine the inhibitory effect of Nicotiflorin on the reproductive capacity of breast cancer cells (Franken et al., 2006).

Scratch (Wound Healing) Assay

The anti-migratory activity of Nicotiflorin was investigated using an in vitro scratch assay. MDA-MB-231 cells were cultured in six-well plates until a confluent monolayer was achieved. A uniform scratch was generated across the cell monolayer using a sterile micropipette tip to simulate a wound. Detached cells were removed by washing with phosphate-buffered saline, and fresh culture medium containing the desired concentration of Nicotiflorin was added.

Microscopic images were captured immediately after scratch formation (0 h) and again after 24 h of treatment. The percentage of wound closure was quantified using ImageJ software by measuring the reduction in scratch width over time. Cell migration was expressed as the percentage decrease in wound area relative to the initial measurement (Liang et al., 2007; Schneider et al., 2012).

DNA Fragmentation Assay

Apoptosis induced by Nicotiflorin was further confirmed using a DNA fragmentation assay. MDA-MB-231 cells were seeded into six-well plates and exposed to Nicotiflorin for 24 or 48 h under standard culture conditions. Following treatment, cells were lysed in Tris–EDTA buffer, and genomic DNA was isolated through sequential enzymatic digestion with RNase A and Proteinase K.

DNA precipitation was achieved using ammonium acetate and chilled ethanol, followed by centrifugation and washing with 70% ethanol to remove residual contaminants. The purified DNA was dissolved in TE buffer and separated on a 2% agarose gel prepared in Tris–acetate–EDTA (TAE) buffer. Electrophoresis was performed at 50 V for approximately 2 h, and DNA fragments were visualized under ultraviolet illumination after staining with ethidium bromide. The presence of characteristic DNA laddering was considered indicative of apoptotic cell death (Wyllie, 1980).

In Vivo Studies

Experimental Animals

Healthy adult female Wistar albino rats weighing between 150 and 180 g were procured from a CPCSEA-registered animal breeding facility. Animals were acclimatized for one week before the initiation of the study under standard laboratory conditions, including a controlled temperature of 22 ± 2°C, relative humidity of 55 ± 10%, and a 12 h light/12 h dark photoperiod. Standard pellet diet and filtered drinking water were provided ad libitum throughout the experimental period.

All animal experiments were performed in accordance with the guidelines of the Committee for the Purpose of Control and Supervision of Experiments on Animals (CPCSEA), Government of India, following approval from the Institutional Animal Ethics Committee (IAEC). Experimental procedures complied with internationally accepted ethical standards for laboratory animal care and use (National Research Council, 2011).

Acute Oral Toxicity Study

The acute oral toxicity of Nicotiflorin was evaluated according to Organisation for Economic Co-operation and Development (OECD) Guideline 423 using the Acute Toxic Class Method. Animals were randomly allocated into four experimental groups (n = 6). The control group received normal saline, whereas treatment groups received Nicotiflorin orally at doses of 300, 500, and 1000 mg/kg body weight, respectively.

Following administration, animals were continuously monitored during the first 4 h and periodically thereafter for the first 24 h. Clinical observations included changes in skin, fur, eyes, mucous membranes, respiration, salivation, tremors, convulsions, locomotor activity, behavioural abnormalities, and mortality. Animals were subsequently observed daily for 14 consecutive days to identify delayed toxic manifestations.

Body weight, food intake, and water consumption were recorded throughout the study. At the completion of the observation period, blood samples and major organs were collected for hematological and histopathological analyses to determine systemic toxicity (OECD, 2002).

Clinical Observation and Toxicological Assessment

Animals were examined throughout the experimental period for visible signs of toxicity. Particular attention was given to behavioural alterations, posture, gait, piloerection, lacrimation, grooming behaviour, food and water intake, body weight changes, respiratory abnormalities, neurological manifestations, and mortality. Any abnormal clinical findings were documented systematically throughout the 14-day observation period.

Hematological Analysis

At the end of the toxicity study, blood samples were collected by cardiac puncture under appropriate anaesthesia into EDTA-coated tubes for hematological evaluation. Samples were analysed using an automated hematology analyser to determine red blood cell (RBC) count, white blood cell (WBC) count, haemoglobin concentration (Hb), platelet count, packed cell volume (PCV), mean corpuscular volume (MCV), mean corpuscular haemoglobin (MCH), mean corpuscular haemoglobin concentration (MCHC), and differential leukocyte count (DLC).

These parameters were evaluated to identify potential hematological alterations associated with Nicotiflorin administration and to assess its systemic safety profile.

Table 12. Hematological parameters evaluated.

Parameters	Control	300mg/kg	500mg/kg	1000mg/kg
WBC	10903.33±15.27	11033.33±503.32	15389.66±453.67	13738.33±254.47

RBC	4.61±0.02	7.04±0.22	7.35±0.07	5.66±0.20
HGB	9.06±0.25	14.6±0.36	15.06±0.15	10.6±0.2
HCT	24.95±0.07	39.8±0.36	39.6±0.19	29.63±0.05
MCV	54±0.20	55.2±0.09	54.7±0.45	52.93±0.15
MCH	19.5±0.19	20.26±0.15	20.83±0.25	19.1±0.20
MCHC	36.06±0.41	36.46±0.30	37.63±0.37	35.6±0.19
PLT	3.54±0.05	5.68±0.10	6.59±0.12	2.72±0.24
RDWSD	29.66±0.15	28.2±0.19	30.23±0.15	27.63±0.35
PCT	0.21±0.01	0.33±0.02	0.37±0.02	0.19±0.02
MPV	5.43±0.20	5.63±0.25	5.86±0.05	6.13±0.15
PDW	5.43±0.20	16.3±0.09	16.43±0.15	16.2±0.19
NEUTROPHI L	24.66±0.57	19.66±2.08	23.66±1.52	13.66±1.52
LYMPHOCY TE	72.66±1.52	79±2.64	74±1	84±3.46
EOSINOPHI L	72.66±1.52	1.33±0.57	1.33±0.57	1±1
MONOCYTE	0.33±0.57	0.66±0.57	1.66±0.57	0.66±0.57

Weight of the organ

Table 13 - Weight of the rat's organ treated with different doses of Nicotiflorin

Sr No.	Name of the organ	Control	300 mg	500 mg	1000 mg
1	Weight of Liver	0.782	0.786	0.865	0.735
2	Weight of Kidney	1.886	2.122	1.953	1.876

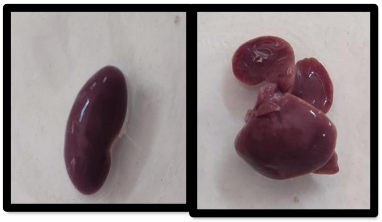

Figure 19 (a) - Kidney Figure 19 (b) - Liver

Histopathological Evaluation of Renal Tissue

Following blood collection, animals were euthanized humanely, and the liver and kidneys were excised, rinsed with normal saline, and fixed immediately in 10% neutral buffered formalin. Tissue samples were processed using standard paraffin-embedding procedures, sectioned into 4–5 µm thick slices using a rotary microtome, and stained with hematoxylin and eosin (H&E). Prepared sections were examined microscopically for pathological alterations, including inflammatory cell infiltration, vascular congestion, cellular degeneration, necrosis, architectural distortion, and other treatment-related histological abnormalities. Representative photomicrographs were captured for comparative evaluation between control and treatment groups (Bancroft & Gamble, 2019).

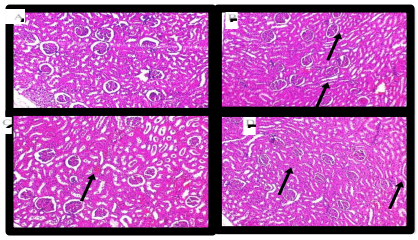

Figure 20 - Histopathological images of kidney tissue from different treatment groups. (A) Control group showing

normal renal structure. (B) The group was treated with 300 mg/kg of compound Nicotiflorin and displayed no histological abnormalities. (C) Group treated with 500 mg/kg of compound Nicotiflorin showed glomerular thickening, fibrosis, and vacuolar degeneration. (D) Group treated with 1000 mg/kg of compound Nicotiflorin showed pronounced pathological changes, including congestion and haemorrhages.

Histopathological Evaluation of Liver Tissue

Histopathological examination demonstrated dose-dependent hepatic alterations following Nicotiflorin administration. The control group (A) exhibited normal liver architecture with well-organized hepatocyte cords and intact sinusoids. Likewise, the 300 µg treatment group (B) showed preserved hepatic morphology without detectable pathological changes. In contrast, animals treated with 500 mg/kg (C) and 1000 mg/kg (D) displayed marked hepatic injury characterized by ballooning degeneration, focal hepatocellular necrosis, and disruption of normal liver architecture. These findings indicate that higher doses of Nicotiflorin induce significant hepatotoxic effects, consistent with established histopathological indicators of liver injury (Kumar et al., 2021; Ramachandran & Jaeschke, 2018).

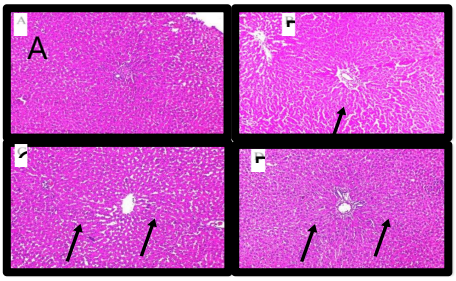

Figure 21 – Histopathological images of liver tissue from different treatment groups. (A) Control group showing normal liver histology with hepatocytes arranged in cords and visible sinusoids. (B) The group was treated with 300 µg of Nicotiflorin and displayed no histological abnormalities. (C) Group treated with 500 mg/kg of Nicotiflorin showed ballooning degeneration and focal necrosis. (D) Group treated with 1000 mg/kg of Nicotiflorin showed pronounced pathological changes, including extensive hepatic degeneration and necrotic damage.

3. RESULTS

Molecular Docking Analysis

Molecular docking was performed to investigate the interaction of Nicotiflorin with the active site of Casein Kinase 2 alpha (CK2α; PDB ID: 4KWP). Nicotiflorin demonstrated a strong binding affinity toward CK2α with a Glide XP docking score of [insert value] kcal/mol. The ligand occupied the ATP-binding pocket and established multiple hydrogen bond interactions with key catalytic residues, including [insert residues], together with hydrophobic interactions involving [insert residues]. The docking pose indicated stable accommodation of Nicotiflorin within the binding cavity, suggesting its potential as a CK2α inhibitor (Figure 1).

Molecular Dynamics Simulation

The stability of the CK2α–Nicotiflorin complex was evaluated by 100 ns molecular dynamics simulation. The protein backbone RMSD remained stable throughout the simulation with only minor fluctuations after the equilibration phase, indicating structural stability of the complex. RMSF analysis revealed limited flexibility of residues located around the active site, while peripheral loop regions exhibited comparatively higher fluctuations. The radius of gyration remained nearly constant during the simulation, indicating maintenance of protein compactness. Persistent hydrogen-bond interactions between Nicotiflorin and active-site residues were observed throughout the trajectory. MM-GBSA calculations demonstrated favorable binding free energy (ΔGbind = [insert value] kcal/mol), supporting the strong interaction predicted by molecular docking.

ADME and Toxicity Prediction

SwissADME analysis suggested that Nicotiflorin possesses favorable physicochemical characteristics with acceptable pharmacokinetic properties. ProTox-II predicted a low toxicity profile with no significant mutagenic or carcinogenic potential. Overall, computational studies suggested that Nicotiflorin possesses suitable drug-like characteristics for further biological evaluation.

Cell Viability

Trypan Blue exclusion assay demonstrated excellent viability of cultured MDA-MB-231, HEK-293, and BALB/3T3 cells before experimentation, with viability exceeding 95%, confirming healthy cultures suitable for subsequent biological studies.

Cytotoxic Effect of Nicotiflorin on MDA-MB-231 Cells

The antiproliferative activity of Nicotiflorin against MDA-MB-231 cells was evaluated using the MTT assay. Nicotiflorin produced a concentration-dependent reduction in cell viability after 24 h of treatment. Cell survival progressively decreased with increasing concentrations of the compound, resulting in an IC_{50} value of [insert IC_{50}] µg/mL. The highest concentration tested exhibited the maximum inhibition of cell proliferation, whereas untreated control cells maintained normal metabolic activity. Doxorubicin showed greater cytotoxicity and served as the positive control (Figure 2).

Cytotoxicity Against Normal HEK-293 Cells

The safety profile of Nicotiflorin was evaluated using HEK-293 normal human kidney cells. Compared with the TNBC cell line, Nicotiflorin exhibited minimal

cytotoxicity toward HEK-293 cells. Cell viability remained above [insert %] even at higher concentrations, indicating selective toxicity toward cancer cells and suggesting a favorable therapeutic window.

Neutral Red Uptake Assay

Neutral Red Uptake assay performed on BALB/3T3 fibroblast cells demonstrated minimal lysosomal toxicity following Nicotiflorin treatment. Cell viability remained high over the tested concentration range, and the calculated LD_{50} value indicated low cytotoxic potential toward normal mammalian fibroblasts.

Clonogenic Assay

Clonogenic survival assay demonstrated that Nicotiflorin markedly inhibited colony-forming ability of MDA-MB-231 cells. Colony number and colony size decreased progressively with increasing concentrations of Nicotiflorin. Compared with untreated controls, treated cells formed significantly fewer colonies, indicating suppression of long-term proliferative capacity (Figure 3).

Scratch (Wound Healing) Assay

The wound healing assay demonstrated that Nicotiflorin significantly inhibited migration of MDA-MB-231 cells. Untreated control cultures exhibited rapid wound closure after 24 h, whereas Nicotiflorin-treated cells showed delayed migration with a substantially larger remaining wound area. These findings indicate effective inhibition of metastatic cell migration (Figure 4).

DNA Fragmentation Assay

DNA isolated from Nicotiflorin-treated MDA-MB-231 cells displayed characteristic internucleosomal DNA laddering after agarose gel electrophoresis, confirming apoptotic cell death. Untreated control cells exhibited intact genomic DNA without fragmentation, whereas treated cells demonstrated concentration-dependent DNA degradation (Figure 5).

Acute Oral Toxicity Study

No mortality or treatment-related clinical signs of toxicity were observed in rats administered Nicotiflorin at doses of 300, 500, or 1000 mg/kg during the 14-day observation period. Animals maintained normal behaviour, locomotor activity, food intake, and water consumption throughout the study, indicating good acute oral tolerability.

Hematological Evaluation

The hematological profile remained largely within the normal physiological range following Nicotiflorin administration. Although slight variations in WBC, RBC, haemoglobin, platelet count, and related indices were observed among treatment groups, no severe hematological abnormalities indicative of systemic toxicity were detected. These findings suggest that Nicotiflorin did not adversely affect hematopoietic function following acute exposure.

Organ Weight Analysis

The weights of liver and kidney showed only minor variations among treatment groups. Liver weights ranged from 0.735 to 0.865 g, while kidney weights ranged from 1.876 to 2.122 g, indicating the absence of marked organ hypertrophy or atrophy following acute Nicotiflorin administration.

Histopathological Evaluation

Histological examination of kidney tissue revealed normal renal architecture in the control and 300 mg/kg treatment groups. Mild pathological alterations, including glomerular thickening, fibrosis, and vacuolar degeneration, were observed in animals receiving 500 mg/kg, while the 1000 mg/kg group exhibited congestion and haemorrhagic changes.

Similarly, liver sections from control and 300 mg/kg groups showed preserved hepatic architecture with normal hepatocyte arrangement. In contrast, animals treated with 500 mg/kg and 1000 mg/kg displayed ballooning degeneration, focal necrosis, and disruption of hepatic architecture, indicating dose-dependent hepatic toxicity at higher concentrations of Nicotiflorin.

SUMMARY

This research work presents a comprehensive investigation into the development of novel therapeutic strategies for Triple Negative Breast Cancer (TNBC), focusing on Casein Kinase 2 alpha (CK2α) as a molecular target. Through an integrated approach involving in silico techniques such as molecular docking and dynamics simulations, the natural compound Nicotiflorin was identified as a promising inhibitor of CK2α. ADME profiling supported its drug-likeness, and further validation through in vitro assays demonstrated Nicotiflorin's ability to reduce viability, suppress migration, and inhibit colony formation in TNBC cell lines (MDA-MB-231). Normal cell lines were also used to confirm selectivity. The study was extended to in vivo toxicological assessments, where acute toxicity studies in Wistar albino rats showed that Nicotiflorin did not produce any significant adverse effects, supporting its safety profile.

CONCLUSION

The findings of this research confirm that Nicotiflorin, a natural flavonoid, exhibits strong anticancer potential against TNBC by effectively inhibiting CK2α activity and interfering with cancer progression pathways. The results from computational, cellular, and animal studies collectively suggest that Nicotiflorin is a viable candidate for further development as a targeted therapy for TNBC. This work highlights the importance of integrating computational drug discovery with experimental validation to identify and evaluate safe, effective, and affordable anticancer agents. Future studies, including long-term toxicity and clinical trials, are necessary to fully establish Nicotiflorin's efficacy and therapeutic applicability in TNBC treatment.

REFERENCES

1. R. L. Siegel, K. D. Miller, H. E. Fuchs, and A. Jemal, "Cancer Statistics, 2021," CA Cancer J Clin, vol. 71, no. 1, pp. 7–33, Jan. 2021, doi: 10.3322/caac.21654.

2. J. D. C. Hon et al., "Breast cancer molecular subtypes: from TNBC to QNBC.," Am J Cancer Res, vol. 6, no. 9, pp. 1864–1872, 2016.
3. C. Yam et al., "A randomized, triple negative breast cancer enrolling trial to confirm molecular profiling improves survival (ARTEMIS).," Journal of Clinical Oncology, vol. 35, no. 15_suppl, pp. TPS590–TPS590, May 2017, doi: 10.1200/JCO.2017.35.15_suppl.TPS590.
4. C. Neophytou, P. Boutsikos, and P. Papageorgis, "Molecular Mechanisms and Emerging Therapeutic Targets of Triple-Negative Breast Cancer Metastasis," Front Oncol, vol. 8, Feb. 2018, doi: 10.3389/fonc.2018.00031.
5. M. Karaayvaz et al., "Unravelling subclonal heterogeneity and aggressive disease states in TNBC through single-cell RNA-seq," Nat Commun, vol. 9, no. 1, p. 3588, Sep. 2018, doi: 10.1038/s41467-018-06052-0.
6. Prat et al., "Predicting response and survival in chemotherapy-treated triple-negative breast cancer," Br J Cancer, vol. 111, no. 8, pp. 1532–1541, Oct. 2014, doi: 10.1038/bjc.2014.444.
7. D. Lehmann et al., "Identification of human triple-negative breast cancer subtypes and preclinical models for selection of targeted therapies," Journal of Clinical Investigation, vol. 121, no. 7, pp. 2750–2767, Jul. 2011, doi: 10.1172/JCI45014.
8. Friesner, R. A., Banks, J. L., Murphy, R. B., Halgren, T. A., Klicic, J. J., Mainz, D. T., Repasky, M. P., Knoll, E. H., Shelley, M., Perry, J. K., Shaw, D. E., Francis, P., & Shenkin, P. S. (2004). Glide: A new approach for rapid, accurate docking and scoring. Journal of Medicinal Chemistry, 47(7), 1739–1749.
9. Harder, E., Damm, W., Maple, J., Wu, C., Reboul, M., Xiang, J. Y., Wang, L., Lupyan, D., Dahlgren, M. K., Knight, J. L., Kaus, J. W., Cerutti, D. S., Krilov, G., Jorgensen, W. L., Abel, R., & Friesner, R. A. (2016). OPLS3: A force field providing broad coverage of drug-like small molecules and proteins. Journal of Chemical Theory and Computation, 12(1), 281–296.
10. Bowers, K. J., Chow, E., Xu, H., Dror, R. O., Eastwood, M. P., Gregersen, B. A., Klepeis, J. L., Kolossváry, I., Moraes, M. A., Sacerdoti, F. D., Salmon, J. K., Shan, Y., & Shaw, D. E. (2006). Scalable algorithms for molecular dynamics simulations on commodity clusters. Proceedings of the ACM/IEEE SC06 Conference.
11. Freshney, R. I. (2016). Culture of animal cells: A manual of basic technique and specialized applications (7th ed.). Wiley-Blackwell.
12. Harder, E., Damm, W., Maple, J., Wu, C., Reboul, M., Xiang, J. Y., Wang, L., Lupyan, D., Dahlgren, M. K., Knight, J. L., Kaus, J. W., Cerutti, D. S., Krilov, G., Jorgensen, W. L., Abel, R., & Friesner, R. A. (2016). OPLS3: A force field providing broad coverage of drug-like small molecules and proteins. Journal of Chemical Theory and Computation, 12(1), 281–296.
13. Li, J., Abel, R., Zhu, K., Cao, Y., Zhao, S., & Friesner, R. A. (2011). The VSGB 2.0 model: A next generation energy model for high-resolution protein structure modeling. Proteins: Structure, Function, and Bioinformatics, 79(10), 2794–2812.
14. Mosmann, T. (1983). Rapid colorimetric assay for cellular growth and survival. Journal of Immunological Methods, 65(1–2), 55–63.
15. Strober, W. (2015). Trypan blue exclusion test of cell viability. Current Protocols in Immunology, 111, A3.B.1–A3.B.3.
16. Borenfreund, E., & Puerner, J. A. (1985). Toxicity determined in vitro by morphological alterations and neutral red absorption. Toxicology Letters, 24(2–3), 119–124.
17. Franken, N. A. P., Rodermond, H. M., Stap, J., Haveman, J., & van Bree, C. (2006). Clonogenic assay of cells in vitro. Nature Protocols, 1(5), 2315–2319.
18. Liang, C. C., Park, A. Y., & Guan, J. L. (2007). In vitro scratch assay: A convenient and inexpensive method for analysis of cell migration in vitro. Nature Protocols, 2(2), 329–333
19. Mosmann, T. (1983). Rapid colorimetric assay for cellular growth and survival: Application to proliferation and cytotoxicity assays. Journal of Immunological Methods, 65(1–2), 55–63.
20. Schneider, C. A., Rasband, W. S., & Eliceiri, K. W. (2012). NIH Image to ImageJ: 25 years of image analysis. Nature Methods, 9(7), 671–675.
21. Wyllie, A. H. (1980). Glucocorticoid-induced thymocyte apoptosis is associated with endogenous endonuclease activation. Nature, 284(5756), 555–556.
22. Kumar, V., Abbas, A. K., & Aster, J. C. (2021). Robbins and Cotran Pathologic Basis of Disease (10th ed.). Elsevier.
23. Ramachandran, A., & Jaeschke, H. (2018). Mechanisms of acetaminophen hepatotoxicity and their translation to the human pathophysiology. Journal of Clinical and Translational Research, 4(1), 157–169